Collaborative Fault Recovery and Network Reconstruction Method for Cyber-physical-systems Based on Double Layer Optimization

Wanxing Sheng, *Senior Member*, *IEEE*, Keyan Liu, *Member*, *IEEE*, Zhao Li, *Member*, *IEEE*, and Xueshun Ye

***Abstract*—For fault characteristics of cyber-physical-systems (CPS) based distribution network, a spatiotemporal incidence matrix to represent correlation of concurrent faults on cyberspace and physical space is proposed, and strategies of fault location, removal, and recovery of concurrent faults are analyzed in this paper. Considering the multiple objectives of minimum network loss, voltage deviation, and switching operation times, a collaborative power supply restoration model of a CPS-based distribution network with the strategy that restoration of the communication layer is prior to the physical layer is constructed using the Dijkstra's dynamic routing algorithm and second-order cone relaxation distribution network reconfiguration method, to realize orderly recovery of a distribution network during CPS concurrent faults. Related investigations are made based on the DCPS-160 case, and the accuracy and effectiveness of the proposed model are also verified.**

***Index Terms*—Collaborative fault, cyber-physical-systems, distribution network, double layer optimization.**

I. Introduction

With rapid development and applications of the Internet of Things, information communication, 5G, and other related technology, the traditional distribution network (DN) has evolved into a multi-level and comprehensive network architecture including a physical layer and a communication layer. Furthermore, the physical layer has more dependence on the communication layer, which has been a typical cyber-physical system (CPS). The CPS is a closed-loop system that has the advantages of situational awareness, real-time analysis, scientific decisions, and precise implementation. Therefore, the DN based on CPS is different from traditional DN reflected in three perspectives, i.e., composition and structure, control mode, and information processing. For composition and structure, the CPS DN pays more attention to the influence of the communication network and multiple information on the physical network, while, the control mode used in the CPS DN is more flexible than that used in traditional DN. Furthermore, the CPS DN can keep compatibility with the communication mode of all kinds of devices and can achieve a high degree of consistency in the integration of system information and coordination in the functionalities of primary and secondary systems.

In terms of the DN fault, there may be faults occurring in the physical layer or communication layer separately, further, it can also be concurrent faults occurring in the physical and communication layers simultaneously. In general, researchers pay attention to the faults in these two layers separately.

A fault occurring in the communication layer is mainly link interruption, data falsification, and control failure, such as communication cable damage, false data injection attacks (FDIAs), man-in-the-middle attacks (MitM), distributed denial of service (DDoS), etc. Communication cable damage induced by natural disasters has been studied in [1], kinds of fault recovery strategies and algorithms were proposed. In addition, a fast fault recovery algorithm of the cyber link in the smart grid had been proposed in [2], the basic process of this algorithm is establishing the backup tree forwarding rules first, and then uploading the fault by OpenFlow, finally repairing the communication topology by calling the REACTIVE algorithm. Focusing on large-scale communication networks, some researchers study single-stage and multi-stage fault recovery algorithms [3], [4]. Maximum recovery of customer service had been set as the objective, and mixed-integer programming was utilized to obtain the recovery strategy in the single-stage fault recovery algorithms. Similarly, the same objective had also been used in the multi-stage method, but the link recovery order had been optimized based on the single-stage method [3], [4].

Compared to research on fault recovery of the communication layer, fault recovery on the physical network is relatively more mature. There are mainly two kinds of methods, which are heuristic algorithm and mathematical optimization algorithm. Commonly used heuristic algorithms include particle swarm optimization algorithm (PSO), genetic algorithm, firefly algorithm, and ant colony algorithm, etc. The recovery strategy of feeder recovery, load transfer, and load shedding using heuristic algorithms was obtained in [5]. For mathematical optimization algorithms, there are mainly three methods, which are mixed-integer linear programming, mixed-integer nonlinear programming, and mixed-integer convex optimization programming [6]–[14]. For instance, the nonlinear power flow

Manuscript received January 2, 2022; revised February 8, 2022; accepted February 23, 2022. Date of online publication August 18, 2022; date of current version December 20, 2022. This work is supported by Funds for International Cooperation and Exchange of the National Natural Science Foundation of China (Grant No. 52061635104, Sustainable urban power supply through intelligent control and enhanced restoration of AC/DC networks).

W. X. Sheng, K. Y. Liu (corresponding author, e-mail: liukeyan@epri.sgcc.com.cn), Z. Li, and X. S. Ye are with China Electric Power Research Institute, Beijing 100192, China.

DOI: 10.17775/CSEEJPES.2022.00040

2096-0042 © 2022 CSEE

equation of DN was relaxed to a second-order cone model by the convex relaxation technique, and the convex optimization algorithm was used to solve the problem. This procedure can guarantee precision and computation speed [11]. Similarly, the same procedure was also used in [12], and the procedure was improved by virtual network theory to enhance computational efficiency. Model construction and solution process in the mathematical optimization algorithm were all based on the mathematical theory and derivation, which made the approach more precise than heuristic algorithms.

The physical layer and communication layer have a high degree of integration with each other in the CPS-based DN, which can significantly enhance fault diagnosis capability. The most commonly used methods of fault diagnosis are the methods based on expert systems, such as artificial neural network or Bayesian network, Petri net, the matrix-based method, and the method based on analytic models. These fault diagnose methods are all related to the information interaction process. For instance, the measurement information and early warning information are set as input parameters, meanwhile, fault diagnosis results are set as the output. Furthermore, the general rule can be obtained by training large amounts of sample data to predict and analyze unknown or unpredictable faults [13], [14]. Considering the uncertainty of the information, a Petri-net-based method using intuitionistic fuzzy set theory was proposed in [15].

It can be seen the physical layer has quite close correlation with the communication layer in the DN, a fault occurring in the communication will lead to the losing control of the DN operation or fault deterioration. For instance, the breaker rejecting action induced by MitM and FDIAs in the communication layer leads to the increment of the short circuit current [16]. In addition, the scene that a DDoS attack occurring in the communication layer causes failure of service restoration was also reported in [17] Based on the fault diagnosis technique and the CPS characteristic, some researchers carried out the methods of fault diagnosis and service restoration of CPS-based DN. Concurrent fault development path and treatment were discussed in the DN after a DDoS attack in [18].

In summary, although attention had been focused on fault analysis in the communication layer, physical layer, and both of them, there are still some shortages. First, most existing research on the communication layer depend on the public communication network, in which flow maximization is set as an objective. However, the communication network in DN is specific, and restoration maximization should be set as an objective to enhance security and reliability. Moreover, the existing research on fault recovery and service restoration are mainly aimed at architecture, modeling, risk assessment, and information attack detection of the DN based on CPS [19]–[26]. However, research on the strategy and algorithm of the cyber-physical concurrent fault recovery are quite extensive. Therefore, concurrent fault recovery of the DN based on CPS is realized in this paper by analyzing the correlation between the physical layer and cyber layer, with consideration of the particularity of CPS.

The remainder of this paper is organized as follows: Section II introduces the types, description method, and recovery strategy of the physical-cyber concurrent fault in detail. In Section III, model construction and double-layer optimization method are proposed based on the strategy mentioned in Section II. Further, the recovery strategy of the physical-cyber concurrent fault is investigated based on standard DN example, i.e. DCPS-160, meanwhile, related parameters and recovery results are also analyzed in Section VI. Finally, the research content is summarized in Section V.

II. Characterization of the Concurrent Fault in CPS based on DN

A. Concurrent Fault Categories of the CPS based DN

The fault may occur in the physical layer and the communication layer at the same time. Among them, the fault that occurs in the physical layer mainly includes three-phase short circuit fault, two-phase short circuit fault, single-phase short circuit fault, interphase short circuit fault, etc. Meanwhile, the fault occurring in the communication layer is generally caused by many reasons, such as transmission fault (i.e. information channel blocked and transmission delay due to the DDoS attack), data error (i.e. bit error caused by communication interference, or the MitM caused by network attack), and control failure.

Superposition of the physical fault and cyber fault will have great influence on fault location, fault isolation, and power supply restoration in the CPS fault recovery process of the distribution network. The schematic diagram of fault disposal processing is shown in Fig. 1. As can be seen, the fault occurs near node 5, shown 1 Fig. 1(a), and the fault information is uploaded to the distribution master station, shown in Fig. 1(b), further, the isolation command is issued by the distribution master station and node 3, 5, and 6 near the fault point loss of the power supply, shown in Fig. 1(c). Finally, the reconfiguration command is issued by the distribution master station, and the power supply of node 7 and its downstream nodes is restored, shown in Fig. 1(d). It can be seen the handling of distribution network faults and the process of power supply restoration are highly dependent on the distribution master station and auxiliary communication system. When the cyber system fails, it may have significant impact on normal operation of the physical system and the fault recovery scene.

B. Concurrent Fault Modeling of Distribution Network based on CPS

In the physical and cyber concurrent fault situation of the distribution network, there are topology and data flow coupling relationships between the physical layer and communication layer. In Fig. 2, taking the DDoS attack scene as an example, the attacker selects router 4 as the attack target, FTU (Feeder Terminate Unit) 1 is the puppet terminate, a large number of useless communication data are sent to router 4 from FTU 1. As it can be seen from Fig. 2, a large number of useless communication data packets will reach router 4 through OLT (Optical Line Terminal) 1, distribution station 1, switch 1, and

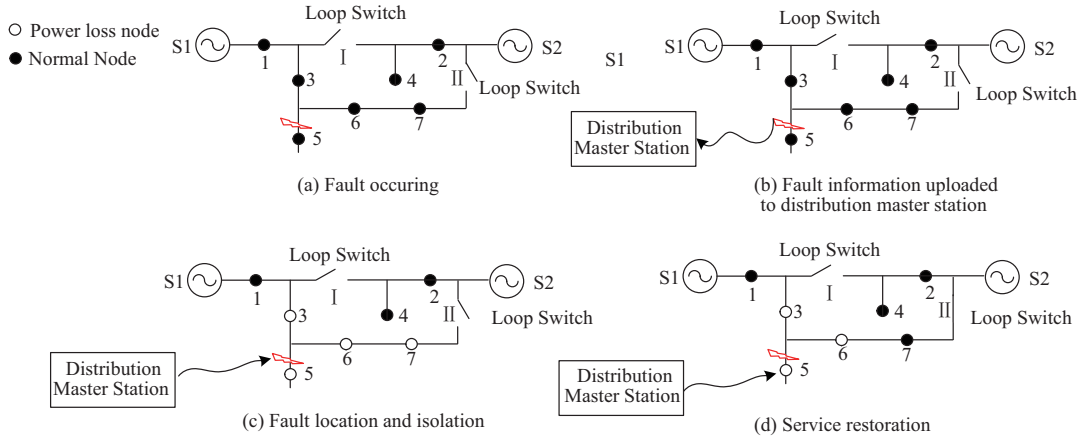

Fig. 1. Schematic diagram of fault disposal processing in the CPS based distribution network.

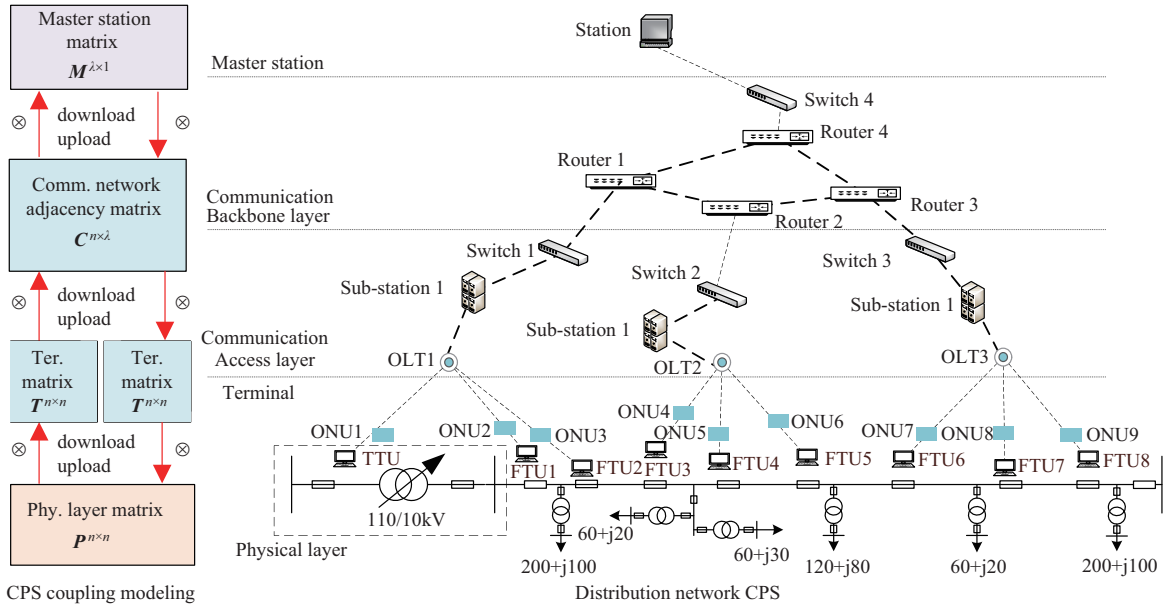

Fig. 2. Characterization of the coupling relationship between the cyber and physics in the distribution network based on CPS.

router 1, router 4 will consume many computing resources to process useless communication data, which will seriously reduce working efficiency of the router. At the same time, the link through FTU 1 to router 4 has a congested state, and other FTUs sharing the communication link to router 4 can't upload or receive information in time. Then, when the physical layer fault occurs, the distribution master station can't receive the fault information uploaded by the FTU or receive fault isolation and recovery strategy commands from the distribution master station. In this state, the power failure load can't be recovered. Thus, it brings security threats to the distribution network.

According to the above analysis, this paper proposes a modeling method based on a spatiotemporal incidence matrix to describe the coupling relationship between the physical layer and communication layer, as shown in (1).

$$\boldsymbol{O}^{n\times 1} = \boldsymbol{P}^{n\times n} \times \boldsymbol{T}^{n\times m} \times \boldsymbol{C}^{m\times m} \times \boldsymbol{M}^{m\times 1} \tag{1}$$

where $\boldsymbol{O}^{n\times 1}$ is spatiotemporal incidence matrix in the distribution network CPS, $\boldsymbol{P}^{n\times n}$ is the physical layer matrix, $\boldsymbol{T}^{n\times m}$ is the secondary equipment matrix composed of measurement and communication terminal, $\boldsymbol{C}^{m\times m}$ is communication network adjacency matrix, $\boldsymbol{M}^{m\times 1}$ is master station matrix, n is the physical layer node number, m is the number of core routers in the communication system.

1) Physical layer matrix $\boldsymbol{P}^{n\times n}$

$$\begin{cases} \boldsymbol{P} = \begin{bmatrix} P_{11} & \cdots & P_{1j} & \cdots & P_{1n} \\ \vdots & & \vdots & & \vdots \\ P_{i1} & \cdots & P_{ij} & \cdots & P_{in} \\ \vdots & & \vdots & & \vdots \\ P_{n1} & \cdots & P_{nj} & \cdots & P_{nn} \end{bmatrix} \\ \boldsymbol{P}_{ij} = [L_{ij}, I_{ij}, BR_{ij}] \end{cases}, \quad i,j \in [1,n] \tag{2}$$

where $\boldsymbol{P}_{ij}$ is an element in the layer matrix, it is composed of L_{ij}, I_{ij}, and BR_{ij}. L_{ij} represents the topological link between nodes i and j, I_{ij} represents fault current, BR_{ij} is the operation state of the breaker.

2) Secondary communication terminal matrix $\boldsymbol{T}^{n\times m}$

DTU, FTU, and other communication terminals are important equipment linking the physical and communication system. They are the key equipment for electrical data acquisition and upload to the communication system, also receiving control commands to control the device in the physical system. The secondary communication terminal node matrix is described in (3):

$$\begin{cases} \boldsymbol{T} = \begin{bmatrix} T_{11} & T_{12} & \cdots & T_{1m} \\ T_{21} & T_{22} & \cdots & T_{2m} \\ \vdots & \vdots & \ddots & \vdots \\ T_{n1} & \cdots & \cdots & T_{nm} \end{bmatrix}, \ i \in [1,n], \eta \in [1,m] \\ \boldsymbol{T}_{i\eta} = [W_{i\eta}, S_{i\eta}, I_{i\eta}, CO_{i\eta}] \end{cases} \tag{3}$$

where $\boldsymbol{T}_{i\eta}$ is the $i\eta$-th element in the secondary communication terminal matrix, which is composed of four variables, $W_{i\eta}$, $S_{i\eta}$, $I_{i\eta}$, and $CO_{i\eta}$. $W_{i\eta}$ represents whether there is a communication terminal η installed at node i of the physical layer. If it is not installed, $W_{i\eta} = 0$, $S_{i\eta}$ represents the operation state of the communication terminal, for normal state, $S_{i\eta} = 1$, $I_{i\eta}$ represents the fault current uploaded by the communication terminal, $CO_{i\eta}$ represents the control command received by the communication terminal i.

3) Communication Network Adjacency Matrix $\boldsymbol{C}^{m\times m}$

The communication network adjacency matrix is used to describe the topology and characteristics of the communication network. For a communication network with m communication nodes, the structure of the matrix $\boldsymbol{C}^{m\times m}$ is shown in (4).

$$\begin{cases} \boldsymbol{C} = \begin{bmatrix} C_{11} & \cdots & C_{1j} & \cdots & C_{1m} \\ \vdots & & \vdots & & \vdots \\ C_{i1} & \cdots & C_{ij} & \cdots & C_{im} \\ \vdots & & \vdots & & \vdots \\ C_{m1} & \cdots & C_{nj} & \cdots & C_{mm} \end{bmatrix}, \ i,j \in [1,m] \\ \boldsymbol{C}_{ij} = [B_{ij}, T_{ij}, P_{Bij}, P_{H_{ij}}] \end{cases} \tag{4}$$

where B_{ij} represents the link between nodes i and j whether it is connected or not, if $B_{ij} = 1$, represents the link is connected; T_{ij} is the communication delay between nodes i and j; P_{Bij} is comminution data package transmission error probability between nodes i and j; P_{Hij} is false data injection attack probability between nodes i and j.

As shown in Fig. 3, the communication backbone network is composed of four routers, communication network adjacency matrix $\boldsymbol{C}^{4\times4}$ is established considering communication delay, link interruption, data transmission error probability, and false data injection attack probability.

$$\begin{cases} \boldsymbol{C}^{4\times4} = \begin{bmatrix} c_{11} & c_{12} & c_{13} & c_{14} \\ c_{21} & c_{22} & c_{23} & c_{24} \\ c_{31} & c_{32} & c_{33} & c_{34} \\ c_{41} & c_{42} & c_{34} & c_{44} \end{bmatrix}, \ i,j \in [1,4] \\ c_{ij} = f(B_{ij}, T_{ij}, P_{Bij}, P_{Hij}) \end{cases} \tag{5}$$

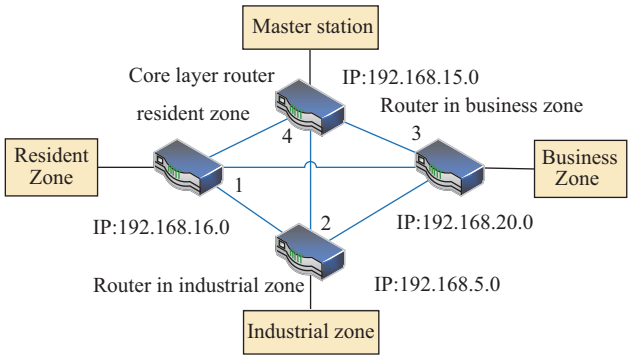

Fig. 3. Communication network topology of four routers.

$$T_{ij} = \begin{cases} 0, & i = j \\ 0.1\ s, & i \neq j \end{cases} \tag{6}$$

$$P_{Mij} = \begin{cases} 0, & i = j \\ 0.01, & i \neq j \end{cases} \tag{7}$$

$$P_{Hij} = \begin{cases} 0, & i = j \\ 0.01, & i \neq j \end{cases} \tag{8}$$

4) Master Station Monitoring and Control Matrix $\boldsymbol{M}^{m\times1}$

The distribution master station is directly connected to the communication layer. It collects data information uploaded by the communication layer to monitor operation of the physical layer. When the fault of the physical layer needs to be handled, it generates control decisions through the fault handling algorithm in the distribution master station, and then sends it to the specific switch of the physical layer through the communication layer for fault isolation and power restoration. In this paper, the master station monitoring and control matrix are described in (9):

$$\begin{cases} \mathrm{Sup}(\boldsymbol{M}) = f_{\text{datadisp}}\left(\sum \boldsymbol{M}_i\right) \\ \mathrm{Con}(\boldsymbol{M}) = f_{\text{opmization}}\left(\sum \boldsymbol{M}_i\right) \end{cases} \tag{9}$$

where $\mathrm{Sup}(\boldsymbol{M})$ and $\mathrm{Con}(\boldsymbol{M})$ represent the monitoring and control functions of the distribution master station, $\boldsymbol{M}_i$ is the data model associated with the communication node i in the distribution master station, and $f_{\text{datadisp}}(\cdot)$ is the operation monitoring processing function; $f_{\text{optimization}}(\cdot)$ is the optimization control processing function.

C. Concurrent Fault Recovery Method of The CPS Based DN

The physical fault recovery method depends on the network reconfiguration function and feeder automation function of the distribution master system. Physical layer network topology reconstruction is realized through the combination of the states of the selection switches and loop switches, to achieve the purpose of load transfer and power supply recovery.

In this investigation, the dynamic routing method is used to handle the fault in the communication layer. The basic rule of this method is that selection of the routers depends on the current state information of the distribution network and communication network. This strategy can better adapt to the changes in communication network traffic and topology and is conducive to improving the performance of the communication

network. The basic process of the dynamic routing method is considering the following three aspects comprehensively, namely, link connectivity, link length, and regional redundancy, and then searching for a link that can recover the biggest fault region, shown in Fig. 4. It can be seen from Fig. 4 that, first, the communication network is abstracted as a graph, meanwhile, all vertices in the graph are divided into two groups, one is the vertices with the known shortest path, named group 1, and the other is the vertices with the unknown shortest path, named group 2. Initially, all vertices belong to group 2, and the path length is set as infinity, meanwhile, the path length of the starting point is set as 0. In each stage, vertices with the shortest path length in group 2 are marked as the vertices with the known shortest path, and then calculate the path length from the vertices to the vertices belonging to group 2. If the obtained path length is shorter than the original length, update the path length of the adjacent vertices, and set the front node of the adjacent vertices as the selected vertices, Loop until the vertices number of group 2 reduces to 0. Finally, the fault recovery strategy of the communication layer can be obtained by outputting the communication routing table.

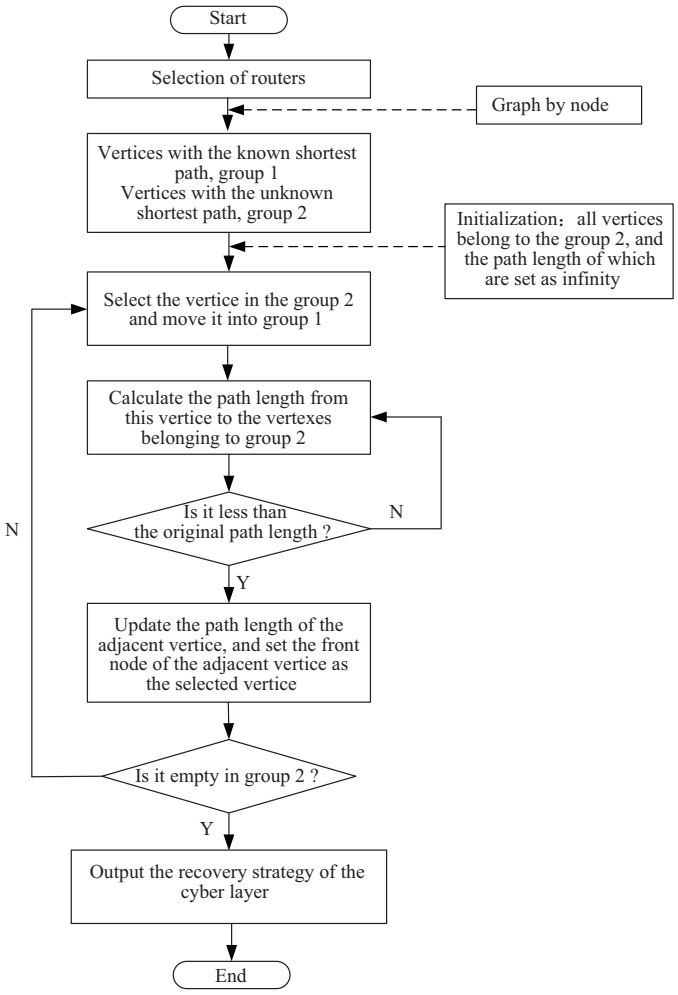

Fig. 4. Dynamic routing method in the communication layer.

III. Double-Layer Optimization Model for Concurrent Fault Recovery in CPS Based DN

Traditionally, influence of the communication layer is not considered in the research on the operation and control in the distribution network. However, with development of the phasor measurement unit (PMU), intelligent terminal, and other primary and secondary integrated devices, more and more information is transferred and processed in the communication layer to ensure controllability and observability of the smart grid, which results in dependence of intelligent distribution network on communication systems becoming significantly improved. Interaction between the communication layer and physical layer should not be ignored during the process of fault isolation and power restoration, therefore, integration of models both of communication layer and physical layer are proposed in this paper.

A. Fault Recovery Model in the Communication Layer

1) Optimization Objective

Communication quality between the physical equipment and the master station, including on-off, delay rate, data error, false data injection, and so on, has an important impact on the dispatching and operation of the distribution network system. Therefore, for fault recovery of communication network, it is to find the link with the minimum delay time, the lowest bit error rate and the lowest probability of false data injection on the premise of the connectivity of the communication network. The objective is shown in (10).

$$\min f_c\left(x_{ij}^C\right)=\phi\sum_{i=1}^{N^C}\sum_{j=1,j\neq i}^{N^C}T\left(x_{ij}^C\right)+\psi\prod_{i=1}^{N^C}\prod_{j=1,j\neq i}^{N^C}\left[P\left(x_{ij}^C\right)+H\left(x_{ij}^C\right)-P\left(x_{ij}^C\right)H\left(x_{ij}^C\right)\right] \tag{10}$$

where x_{ij}^C represents the on-off state of the link between node i and node j in the communication network, which is the control variable, the value is 0 or 1. When $x_{ij}^C=0$, it represents the link is off, when $x_{ij}^C=1$, it represents the link is on. N^C is the node number of the communication network. $T(x_{ij}^C)$ is the time delay of the link x_{ij}^C. $P(x_{ij}^C)$ is the data error rate. $H(x_{ij}^C)$ is the probability of false data injection. φ and ψ is the weight factor.

2) Constraints

a) Link capacity constraint: Data flow on any communication link should be less than its maximum carrying capacity.

$$p\left(x_{ij}^C\right)\leq p_{ij}^{\max} \tag{11}$$

where $p\left(x_{ij}^C\right)$ represents the data flow of communication link x_{ij}^C, $p_{ij}^{\max}$ is the maximum carrying capacity of communication link x_{ij}^C.

b) Connectivity constraint: The connectivity of communication links depends on two aspects: one is the data link is connected, and the other is nodes on the communication link are available. Any failure of the communication link and nodes will lead to non-satisfaction of the connectivity constraint. This constraint can be expressed in (12):

$$\begin{cases} x_{ij}^C=0B\left(x_{ij}^C\right)=0\left|N_i^C=0\right|N_j^C=0 \\ x^C\in G \end{cases} \tag{12}$$

where $B(x_{ij}^C) = 0$ represents the on-off state of the link x_{ij}^C; $N_i^C = 0$ represents the upstream node i of link x_{ij}^C is in fault state; $N_j^C = 0$ represents the downstream node j of link x_{ij}^C is in fault state; x^C is the link set of all available x_{ij}^C; G represents connectivity constraint from communication terminals to master station.

The recovery model of the communication network is solved by the dynamic routing algorithm based on Dijkstra. The solution algorithm is shown in Algorithm 1. The communication network is abstracted as a graph composed of vertices and branches. The node-set of the path that minimizes the objective function is solved as the routing link for communication ion network recovery link.

Algorithm 1: The pseudocode of the dynamic routing algorithm

Initialization:
$N_i^C = \{G\}$
for *all nodes* N_j^C **do**
  if N_j^C *adjacent to* **then**
    $x_{ij}^C = 1$
    $f_d(j) = c(i,j) = \phi \sum_{i=1}^{N^c} \sum_{j=1,j\neq i}^{N^c} T\left(x_{ij}^C\right) + \psi \prod_{i=1}^{N^c} \prod_{j=1,j\neq i}^{N^c} [P\left(x_{ij}^C\right) + H\left(x_{ij}^C\right) - P\left(x_{ij}^C\right) H\left(x_{ij}^C\right)]$
  else
    $f_d(j) =$ infinity
  end
end
Loop
  find N_j^C not in N_i^C such that $f_d(j)$ is minimum
  add N_j^C to G
  update $f_d(j)$ for all N_j^C adjacent to N_i^C and not in G, and $p\left(x_{ij}^C\right) \leq p_{ij}^{\max}$
  $f_d(j) = \min\left(f_d(j), f_d(j) + c(i,j)\right)$
until *all nodes in* N^C;

B. Fault Recovery Model in the Physical Layer

The fault that occurs in the physical layer of the distribution network will lead to power loss in some areas. Under the premise that capacity provided by the superior power grid is abundant, if connectivity of the distribution network after fault recovery can be guaranteed, power loss load can be fully recovered. Based on this circumstance, operation cost and power supply quality should be taken into consideration to set the objective function. For instance, reducing the frequency of switch operations in the reconstruction process can prolong the service life of the switch to improve economic benefits. Meanwhile, if network loss can be reduced after reconstruction, expenditure of the power grid company can also be reduced. Finally, considering the safety and reliability of the grid, the minimization of voltage deviation should also be set as the objective function, which can also reduce loss on the consumer side.

1) Objective Function

Minimization of network loss, number of switch operations, and voltage deviation is set as the objective function, shown in (13),

$$f_p(x^p) = \min\left(\alpha \sum_{i=1}^{nl} L_{\text{loss}}^i(x^p) + \beta\left(\sum_{k=1}^{m}(1 - Y_k(x^p)) + \sum_{j=1}^{n} Z_j(x^p)\right) + \gamma \sum_{m=1}^{nb} \frac{(V_m(x^p) - V_0)^2}{V_0^2}\right) \tag{13}$$

where x^p represents the switch state, L_{loss}^i represents the network loss of the branch i, Y_k and Z_j demonstrate the state of the section switch and the loop switch after reconfiguration, respectively, m and n represent the number of the section switch and the loop switch, V_a and V_0 demonstrate the voltage of node a and the reference voltage, nb represents the total number of nodes in the physical layer, α, β, and γ demonstrate the weight of the network loss, frequency of switch operation, and voltage deviation.

2) Constraints

a) Power flow constraint: The Distflow model based on second-order cone relaxation is used in the power flow, and Ohm's law-based voltage drop, power balance equations of each node are shown in (14) based on the branch of distribution network shown in Fig. 5.

$$\begin{cases} U_i - U_j = Z_{ij} I_{ij} \\ S_{ij} = U_i I_{ij}^* \\ \sum_{k:k\to i}\left(S_{ki} - Z_{ki}|I_{ki}|^2\right) + s_i = \sum_{j:i\to j} S_{ij} \end{cases} \tag{14}$$

where U_i and U_j represent the voltage of node i and node j, S_{ij} and I_{ij} represent apparent power and current of the branch from node i to node j, respectively. S_{ki}, Z_{ki}, and I_{ki} represent apparent power, impedance, and current of the branch from node k to node i, s_i represents the power capacity access in node i.

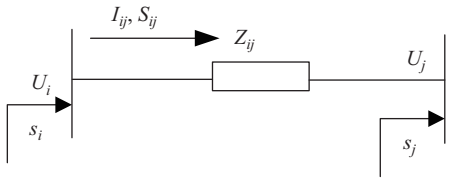

Fig. 5. Branch of distribution network.

Let $P_{ij}+jQ_{ij} = S_{ij}$, $u_i = |U_i|^2$, $\ell_{ij} = |I_{ij}|^2$, and $p_i+jq_i = s_i$, the (14) can be derived to (15) and (16).

$$\begin{cases} \sum_{k:k\to i}(P_{ki} - r_{ki}\ell_{ki}) + p_i = \sum_{j:i\to j} P_{ij} \\ \sum_{k:k\to i}(Q_{ki} - x_{ki}\ell_{ki}) + q_i = \sum_{j:i\to j} Q_{ij} \end{cases} \tag{15}$$

$$\ell_{ij} = \frac{P_{ij}^2 + Q_{ij}^2}{u_i} \tag{16}$$

where P_{ij} and Q_{ij} represent the active power and reactive power of the branch from node i to node j, p_i and q_i demonstrate the active power and reactive power of the power supply access in node i. r_{ki} and x_{ki} represent the resistance and reactance. For the quadratic nonlinear equation (16), the standard second-order cone form of inequality constraints is

obtained by relaxing it through the second-order cone theorem, shown in (17).

$$\frac{P_{ij}^2+Q_{ij}^2}{u_i} \le \ell_{ij} \Leftrightarrow \left\| \begin{bmatrix} 2P_{ij} \\ 2Q_{ij} \\ \ell_i - u_i \end{bmatrix} \right\|_2 \le \ell_i + u_i \tag{17}$$

b) Topology Reconfiguration Constraint: After service restoration, radial topology should be ensured in the distribution network. Therefore, the topology reconfiguration constraint is provided by the fictitious flow method, shown in (18) to (20). Among them, (18) represents the topology tree decoupling constraint of the distribution network, which can guarantee connectivity of the distribution network, and N demonstrates the total number of nodes. Equation (19) represents the KCL constraint to the fictitious flow, while S_{ij} and F_i represent the outflow and inflow of node i. Equation (20) represents the big M method constraint, in which the M is a quite large value. If the branch is interrupted, x_{ij} equals 0, while the branch is connected, x_{ij} equals 1. These two circumstances, both, can meet the constraint. The basic process of the topology reconfiguration and service restoration is shown in Fig. 6, and the corresponding algorithm is shown in Algorithm 2.

$$\sum_{i,j=1}^{N} x_{ij} = |N| - 1 \tag{18}$$

$$\sum_{j:i\to j} S_{ij} + F_i = \sum_{k:k\to i} S_{ki},\ i,j,k \in N/r \tag{19}$$

$$S_{ij} \le (1 - x_{ij})M \tag{20}$$

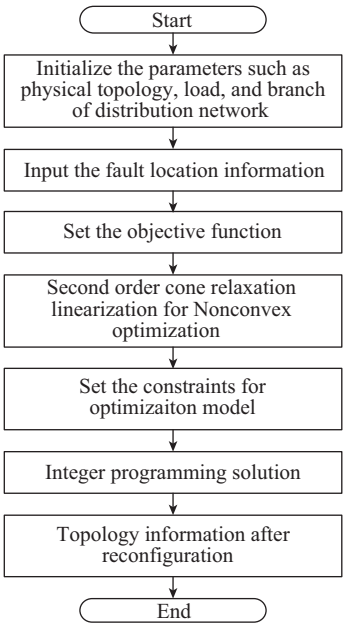

Fig. 6. Procedure of topology reconfiguration and service restoration in the physical layer.

Algorithm 2: Pseudocode of the failure recovery reconfiguration in distribution network using convex optimization method

Input: Distribution network topology, load, branch impedance, and failure position.

Output: Optimal distribution network topology and operation parameters

1 Set virtual flow matrix upstream(nb,nl) and dnstream(nb,nl);
2 Set constraints[], including network topological constraint, power flow constraints, Ohm's law constraints, second-order cone constraints and general constraints.
3 Set objective function, including min(network loss), min(Number of switching actions) and min(voltage deviation), i.e. objective = min(sum(Ploss+N+deV));
4 Set integer linear programming solver, and return Z_{ij} (switch status)

C. Double-Layer Optimization Model for Concurrent Faults

When a physical-cyber concurrent fault occurs in the distribution network system, the distribution master station will lose monitoring, control of the distribution network which will greatly inhibit the ability of the distribution master station to judge network faults and provide recovery strategies. Meanwhile, it is also difficult to execute topology reconstruction instructions effectively. Therefore, a double-layer optimization-based fault recovery method has been proposed to solve the concurrent fault problem. In this method, the upper layer fault, namely the communication layer fault, is recovered to the greatest extent first, and then the obtained communication network topology is substituted into the lower layer, namely physical layer model for physical topology reconstruction, to restore the power supply of distribution network system to the greatest extent.

1) Objective Function

The objective function of the double-layer optimization-based fault recovery method is shown in (21).

$$\begin{cases} \text{upper:} \\ \quad \min f_c\left(x^C\right) \\ \quad \text{s.t. } p\left(x^C\right) = 0 \\ \qquad q\left(x^C\right) \le 0 \\ \text{lower:} \\ \quad f_p\left(x^P, x_{\min}^C\right) \\ \quad x_{\min}^C = \arg\min f_c\left(x^C\right) \\ \quad \text{s.t. } g\left(x^P, x^C\right) = 0 \\ \qquad h\left(x^P, x^C\right) \le 0 \\ \qquad cp\left(x^P, x_{\min}^C\right) = 0 \end{cases} \tag{21}$$

where $f_c(x^{\mathrm{c}})$ represents the objective function of the upper layer optimization model, x^C represents optimization variable of the upper layer, $p(\mathrm{c})$ and $q(\mathrm{c})$ demonstrate equality constraint and non-equality constraint of the upper layer. $f_p(x_p, x_{\min}^C)$ represents the objective function of the lower layer optimization model, and x^P represents the optimization variable of the lower layer. $x_{\min}^C = \arg\min f_c(x^C)$ demonstrates the recovery strategy of the upper layer. $g(x^P, x_{\min}^C)$

and $h(x^P, x^C_{\min})$ represent the equality constraint and non-equality constraint of the lower layer optimization model. $cp(x^P, x^C_{\min})$ demonstrates physical-cyber coupled constraint.

2) Physical-cyber Coupled Constraint

In the CPS-based distribution network, the collected data of the physical layer needs to be uploaded to the distribution master station through the communication layer for fault reconstruction. When the communication node is normal, the corresponding node in the physical layer can be completely acquainted and controlled. Adversely, the corresponding node in the physical layer will be out of control in the circumstance that the communication node is in a fault state.

$$\begin{cases} cp\left(x^P, x^C_{\min}\right) = s\left(x^P | x^C_{\min}\right) = 1 \\ s\left(x^P | x^C_{\min}\right) = \begin{cases} 1, & B\left(x^C_{\min}\right) = 1 \& \sum T\left(x^C_{\min}\right) \le 10s \\ & \& \sum P_{\mathrm{B}}\left(x^C_{\min}\right) \le 0.1 \\ & \& \sum P_{\mathrm{H}}\left(x^C_{\min}\right) \le 0.1 \\ 0, & \text{otherwise} \end{cases} \end{cases} \tag{22}$$

where $s\left(x^P \mid x^C_{\min}\right)$ represents the enable signal of the switch x^P_j. When $s\left(x^P \mid x^C_{\min}\right)$ equals 1, the corresponding switch is controllable, while $s\left(x^P \mid x^C_{\min}\right)$ equals 0 represents the corresponding switch is out of control. $B\left(x^C_{\min}\right)$ represents the link state after recovery, $T\left(x^C_{\min}\right)$ represents the delay of the corresponding link, $P_{\mathrm{B}}\left(x^C_{\min}\right)$ represents the error rate, and $P_{\mathrm{H}}\left(x^C_{\min}\right)$ represents the probability of FDIAs. The basic process of the double layer optimization model is shown in Fig. 7.

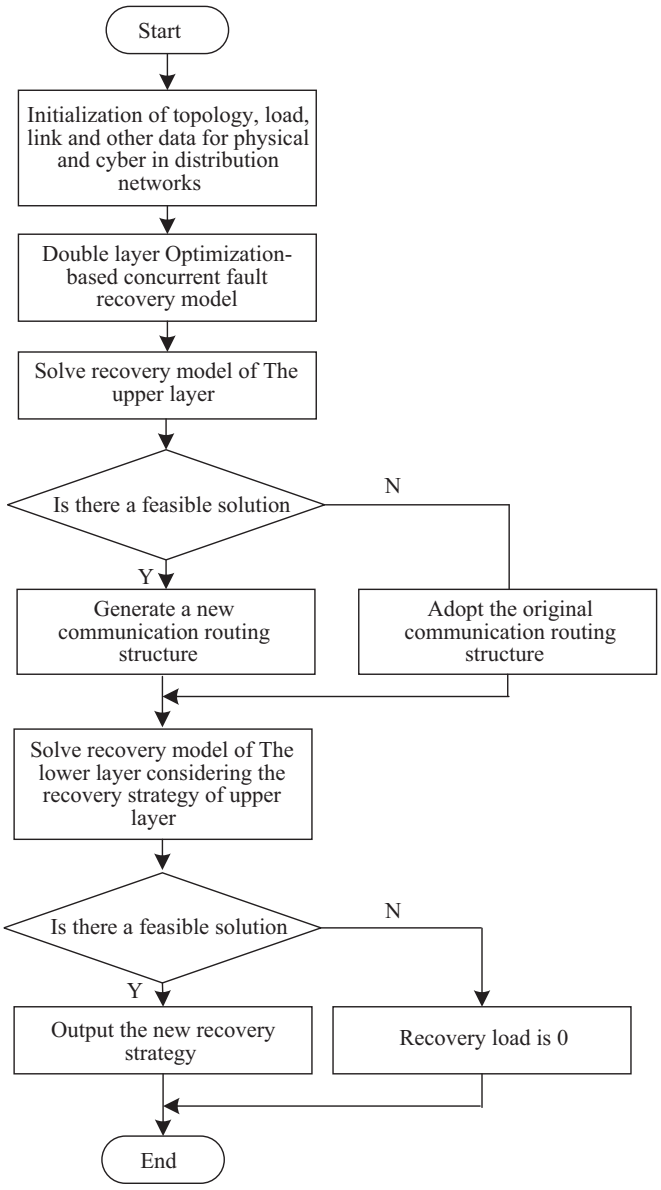

Fig. 7. Solution process of fault recovery.

IV. Experiments and Results

A. Experimental Setting

The algorithm is developed in MATLAB R2021a and runs on an Intel Core i7-10875H 4.5GHz notebook with 16 GB of RAM. Further, the CPLEX solver based on the YALMIP toolbox is carried out to solve the second-order cone optimization problem involved in the fault recovery algorithm. Meanwhile, the topology model of the case is built in Simulink to verify the feasibility and accuracy of the fault recovery strategy.

The investigation in this paper is based on the case DCPS-160, and the topology of the physical layer and communication layer are shown in Fig. 8. Moreover, the details about the case DCPS-160 can be found in [27], [28]. In the physical layer of the DCPS-160 test case, S1, S2, and S3 are power points, 62-2, 42-1, 39-1, 29-1, 35-1, and 13-3 are tie switches, PV2 and PV3 are the photovoltaic generation, dfig2 and dfig3 are the doubly fed fans, BAT1, BAT2 and BAT3 are the battery energy storage devices, gas is the gas turbine and water is the water turbine. Nodes 1∼22 are in the industrial area subnet, nodes 23∼42 are in the residential area subnet, and nodes 43∼62 are in the commercial area subnet. The communication layer of DCPS-160 example includes 4 router nodes, 5 switch nodes, 1 server node, 2 STIL modules, several terminal nodes and communication links. Among them, three routers (i.e. nodes 1∼3) simulate three distribution stations together with four connected switch nodes (DTU1, DTU23, DTU43 and DTU5) respectively, which correspond to three areas on the physical layer. The other router node 4 and switch (FTU26) are used to collect information of three substations and communicate with the master station. Introduction of the communication layer. In addition, the base value and voltage, in this case, are 10 MVA and 10.5 kV, respectively.

B. Comparisons and Discussions

1) Scenario 1

In this scene, the three-phase short circuit fault occurs between node 3 and node 4 at 0.5 s, while the communication layer operates normally. The recovery strategy and results are shown in Table I and Fig. 9. As can be seen, the loss of load is 1884 kW when the fault occurs. After topology reconfiguration according to the recovery strategy, which is opening the section switch 1, 7, and 36, meanwhile, closing the loop switch 42-1, 39-1, 29-1, and 13-3, and all power supplies are restored. In addition, network loss and voltage deviation are both less than those of the original topology.

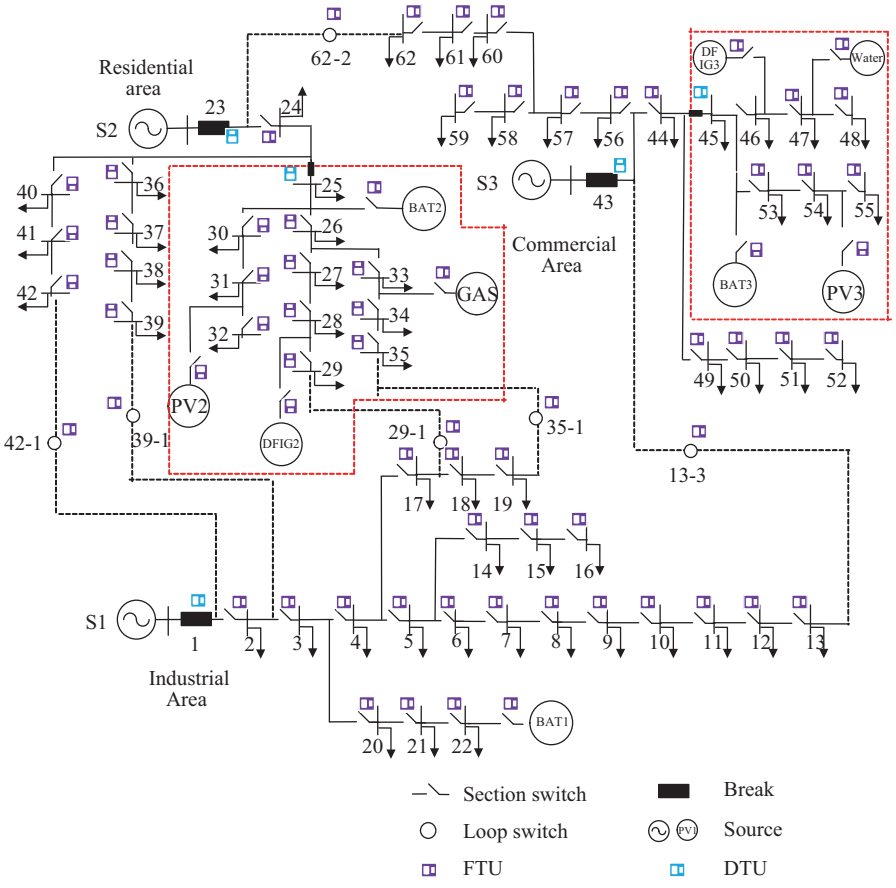

(a) Physical layer

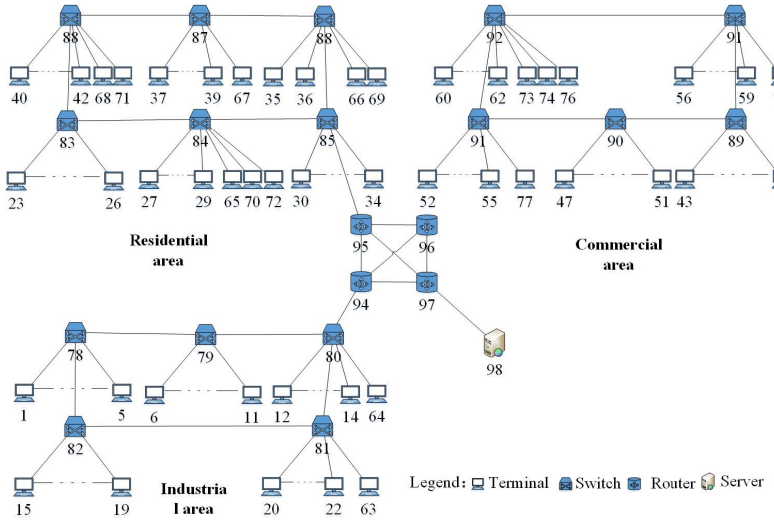

(b) Communication layer

Fig. 8. The topology of case DCPS-160.

TABLE I
PHYSICAL LAYER RECONFIGURATION IN SCENARIO 1

Description	Network topology	Loss of load (kW)	Network loss (kW)	Voltage deviation ($\times 10^{-4}$)	Frequency of switching actions
Fault occurring	Section switch 3 and 4 are open since fault isolation, all loop switch are open	1884	290	13	–
After recovery	Opening the section switch 1, 7, and 36, closing the loop switch 42-1, 39-1, 29-1, and 13-3	0	190	3.76	7
Time (s)				8.03	

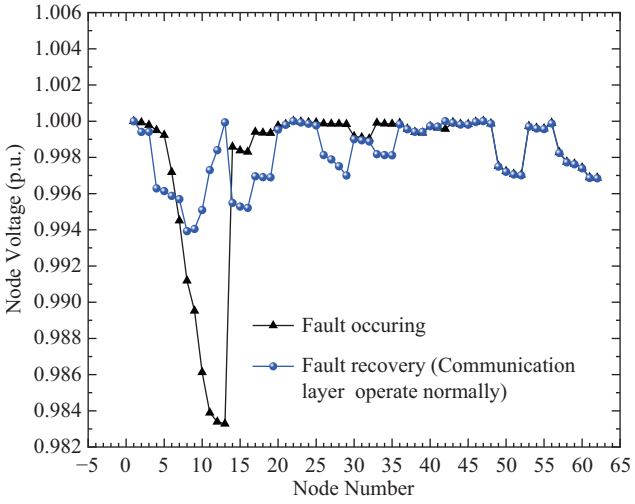

Fig. 9. Node voltage magnitudes in Scenario 1.

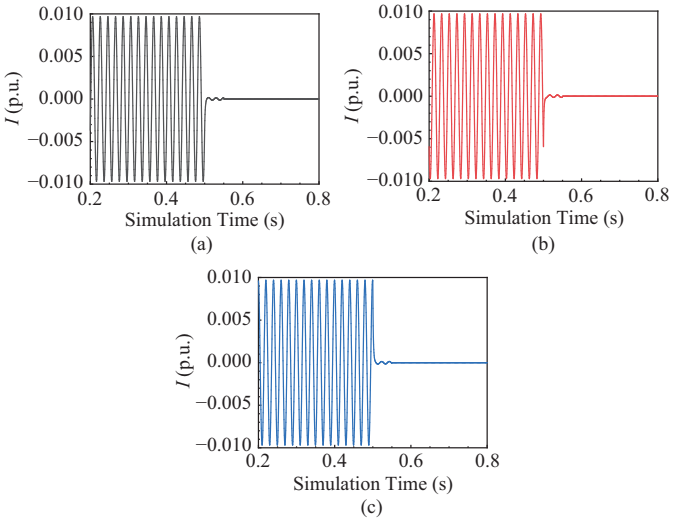

Fig. 10. The current waveform of Node 5 in Scenario 1. (a) Phase A. (b) Phase B. (c) Phase C.

Moreover, the current waveform of Node 5 is observed, shown in Fig. 10. Since node 5 is downstream of the point of failure, current decreases rapidly, which can verify the effectiveness and superiority of the fault recovery strategy.

2) Scenario 2

In this scene, the three-phase short circuit fault occurs between node 3 and node 4 at 0.5 s, meanwhile, the communication layer is attacked by DDoS. In this circumstance, the data background traffic is increased, which leads to data transmission delay increase to 2.5 s, 2.0 s, and 8.9 s for T14, T24, T34 in this area. Meanwhile, there occurs a sharp increase in the bit error rate of the link between the industrial area router and core layer router, and the data transmission error rate is 80%, namely, the PM34 = 0.8. Recovery results of the communication layer are shown in Table II. Table II shows the link channel has changed, and total communication delay time has reduced from 18.4 s to 3.8. Meanwhile, data error rate reduced from 80.6% to 4.9%. In summary, the recovery strategy used in this investigation is feasible and effective.

Although the fault in the communication layer has recovered, there is still extra communication delay, which leads to duration of service restoration extending to 11.83 s. Recovery results in the physical layer are the same as in Scene 1, shown in Table III and Fig. 11, and the current waveform of Node 5 is observed and shown in Fig. 12.

3) Scenario 3

In this Scene, the three-phase short circuit fault occurs between node 3 and node 4 at 0.5 s, at the same time, the fault that denied service occurred at FTU 29-1, which means the loop switch 29-1 cannot execute the instruction issued by the distribution automation system. In this circumstance, the fault information of FTU 29-1 is uploaded to the distribution master system, and the new recovery strategy is generated considering the fault information of the FTU 29-1. The recovery strategy and results at these two conditions, i.e. the condition considering communication layer constraint (named condition 1) and the condition neglecting the fault information of FTU 29-1 (named condition 2), are shown in Table IV and Fig. 13. As can be seen, although the voltage profile of condition 1 is worse than of condition 2, the recovery strategy in condition 1 can restore all power supply in the topology, while there is

TABLE II
COMMUNICATION LAYER RECONFIGURATION IN SCENARIO 1

Description	Link channel	Delay	Interrupt	Data transmission error rate (%)	Probability of data tampering (%)
Fault occurring	(D1, F2, . . ., F-B1)-router-convergence layer router-industrial area router-core layer router-distribution master system	18.4 s	No	80.6	3.9
After recovery	(D1, F2, . . ., F-B1)-router-convergence layer router-industrial area router-residential router-core layer router-distribution master system	3.8 s	No	4.9	4.9

TABLE III
PHYSICAL LAYER RECONFIGURATION IN SCENARIO 3

Description	Network topology	Loss of load (kW)	Network loss (kW)	Voltage deviation ($\times 10^{-4}$)	Frequency of switching actions
Fault occurring	Section switch 3 and 4 are open since fault isolation, all loop switch are open	1884	290	13	–
After recovery	Opening the section switch 1, 7, and 36, closing the loop switch 42-1, 39-1, 29-1, and 13-3	0	190	3.76	7
Time (s)				11.83	

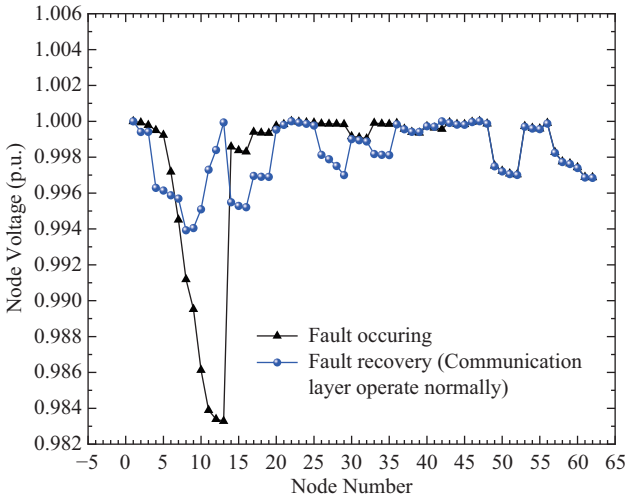

Fig. 11. Node voltage magnitudes in Scenario 2.

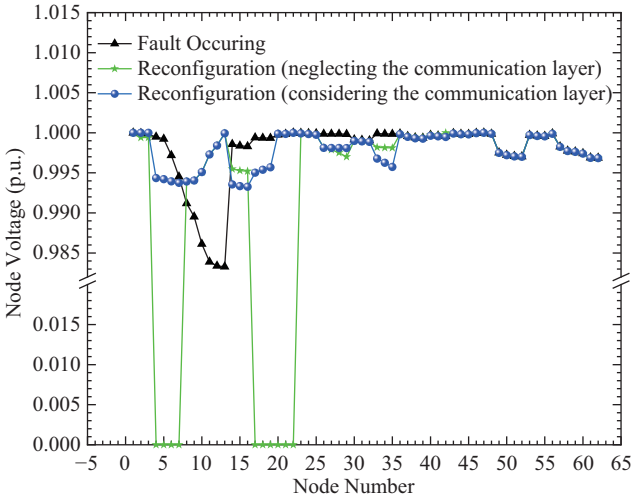

Fig. 13. The current waveform of Node 5 in Scenario 3.

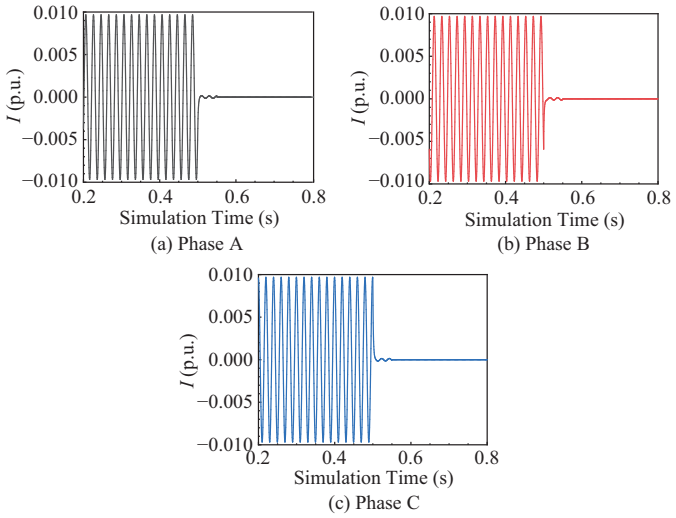

Fig. 12. The current waveform of Node 5 in Scenario 2.

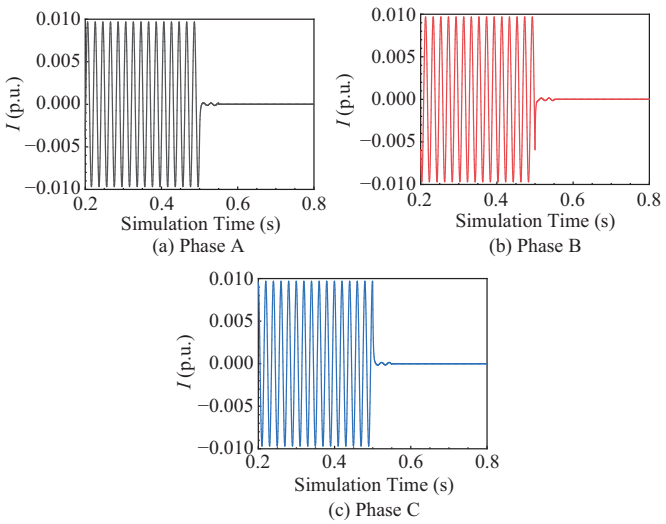

Fig. 14. The current waveform of Node 5 in Scenario 3.

still much loss of load with 524 kW in condition 2. As we all know, the most important objective is to guarantee the quality of power supply in the distribution network area, hence the recovery strategy in condition 1 is reasonable and necessary. The current waveform of node 5 is observed and shown in Fig. 14.

4) Scenario 4

In this scene, the three-phase short circuit fault occurs between node 3 and node 4 at 0.5 s, at the same time the disconnection fault occurs between node 40 and node 41 caused by construction. Simultaneously, there are also faults occurring in the communication layer, that is the link between the industrial area router and core layer router is interrupted, and the link of FTU 29–1 is also interrupted. According to the double-layer optimization theory, the fault in the communication layer is recovered first, and the reconfiguration results of the communication layer are shown in Table V. As can be seen, the communication link has changed, the information can

TABLE IV
PHYSICAL LAYER RECONFIGURATION IN SCENARIO 3

Description	Network topology	Loss of load (kW)	Network loss (kW)	Voltage deviation ($\times 10^{-4}$)	Frequency of switching actions
Fault occurring	Section switch 3 and 4 are open since fault isolation, all loop switches are open	1884	290	13	–
After recovery (neglecting the communication layer)	Opening the section switch 1, 7, and 36, closing the loop switch 42-1, 39-1, 29-1 (rejection), and 13-3	524	–	–	–
After recovery (considering the communication layer)	Opening the section switch 7, closing the loop switch 35-1, and 13-3	0	330	5.78	4
Time (s)				8.05	

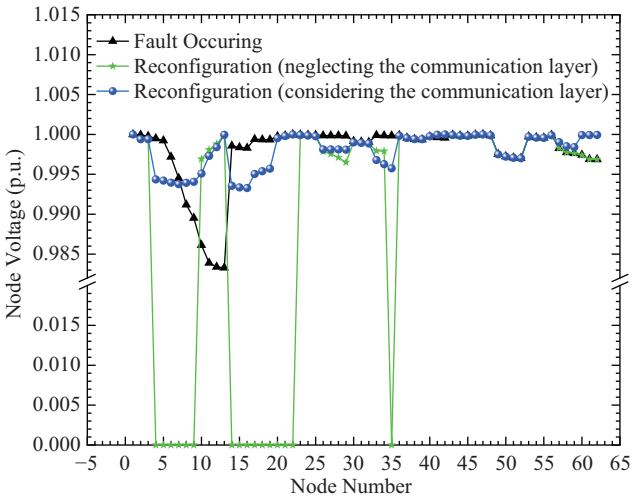

Fig. 15. Node voltage magnitudes in Scenario 4.

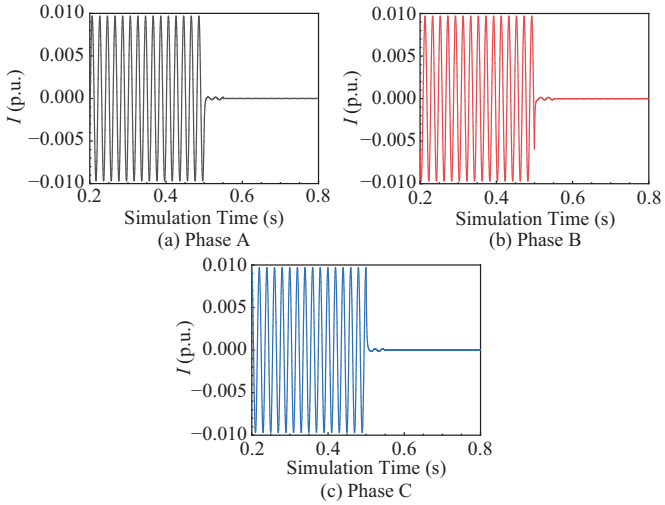

Fig. 16. The current waveform of Node 5 in Scenario 4.

be transmitted over the commercial router and the interrupted link is avoided. Based on the reconfiguration result in the communication layer, the fault recovery strategy and results in the physical layer are obtained, shown in Table VI and Fig. 15. Fig. 16 shows all power supplies are restored, and network loss and voltage deviation are better than before the fault occurs. In addition, there will be more loss of load if the fault in the communication layer is neglected although the voltage profile is better. Results prove the effectiveness and superiority of the recovery strategy provided in this research again.

V. Conclusion

Considering the concurrent fault effect of the physical layer and communication layer, a fault recovery model based on CPS is proposed, and a collaborative recovery method is further put forward in this paper. The following conclusions are described:

1) The incidence matrix of CPS can realize the coupling relationship of fault processing between the physical layer and communication layer, and it can quantitatively reflect the influence range and degree of communication link interruption, delay, bit error, and other faults on power supply restoration, to provide a decision-making basis for the disposal of concurrent faults of distribution network CPS.

2) The recovery model of concurrent faults in CPS-based DN is a multi-objective, multiple constraints, and nonlinear problem. The upper communication recovery model and the lower physical layer model are integrated through the double-layer optimization model. Coupling constraints are adopted between the two layers. The double-layer optimization model is solved based on communication dynamic routing and physical layer second-order cone optimization. Experiments with different scenarios based on the CPS-160 test case show the collaborative recovery method can realize concurrent faults recovery.

TABLE V
Communication Layer Reconfiguration in Scenario 4

Description	Link channel	Delay	Interrupt	Data transmission error rate	Probability of data tampering
Fault occurring	(D1, F2, . . ., F-B1)-router-convergence layer router-industrial area router-core layer router-distribution master system	Interrupted	Yes	Interrupted	Interrupted
After recovery	(D1, F2, . . ., F-B1)-router-convergence layer router-industrial area router-commercial area router-core layer router-distribution master system	0.8 s	No	4.9%	4.9%

TABLE VI
Physical Layer Reconfiguration in Scenario 4

Description	Network topology	Loss of load (kW)	Network loss (kW)	Voltage deviation ($\times 10^{-4}$)	Frequency of switching actions
Fault occurring	Section switch 3 and 4 are open since fault isolation, all loop switch are open	1884	290	13	–
After recovery (neglecting the communication layer)	Opening the section switch 1, 9, and 33, closing the loop switch 42-1, 39-1, 29-1 (rejection), 35-1, and 13-3	1494	–	–	–
After recovery (considering the communication layer)	Opening the section switch 1, 7, and 57, closing the loop switch 42-1, 39-1, 62-2, 35-1, and 13-3	0	200	5.41	4
Time (s)				10.05	

REFERENCES

[1] C. Haseltine and E. E. S. Eman, "Prediction of power grid failure using neural network learning," in *2017 16th IEEE International Conference on Machine Learning and Applications (ICMLA)*, Cancun, Mexico, 2017, pp. 505–510.

[2] D. Gyllstrom, N. Braga, and J. Kurose, "Recovery from link failures in a smart grid communication network using OpenFlow," in *2014 IEEE International Conference on Smart Grid Communications*, 2014, pp. 254–259.

[3] H. F. Yu and C. X. Yang, "Partial network recovery to maximize traffic demand," *IEEE Communications Letters*, vol. 15, no. 12, pp. 1388–1390, Dec. 2011.

[4] S. Kaptchouang, I. A. Ouédraogo, and E. Oki, "Preventive start-time optimization of link weights with link reinforcement," *IEEE Communications Letters*, vol. 18, no. 7, pp. 1179–1182, Jul. 2014.

[5] Y. Y. Hsu, H. M. Huang, H. C. Kuo, S. K. Peng, C. W. Chang, K. J. Chang, H. S. Yu, C. E. Chow, and R. T. Kuo, "Distribution system service restoration using a heuristic search approach," *IEEE Transactions on Power Delivery*, vol. 7, no. 2, pp. 734–740, Apr. 1992.

[6] B. Chen, Z. G. Ye, C. Chen, and J. H. Wang, "Toward a MILP modeling framework for distribution system restoration," *IEEE Transactions on Power Systems*, vol. 34, no. 3, pp. 1749–1760, May 2019.

[7] M. Al Owaifeer and M. Al-Muhaini, "MILP-based technique for smart self-healing grids," *IET Generation, Transmission & Distribution*, vol. 12, no. 10, pp. 2307–2316, May 2018.

[8] M. Ott, M. AlMuhaini, and M. Khalid, "A MILP-based restoration technique for multi-microgrid distribution systems," *IEEE Access*, vol. 7, pp. 136801–136811, Sep. 2019.

[9] S. Khushalani, J. M. Solanki, and N. N. Schulz, "Optimized restoration of unbalanced distribution systems," *IEEE Transactions on Power Systems*, vol. 22, no. 2, pp. 624–630, May 2007.

[10] P. L. Cavalcante, J. C. López, J. F. Franco, M. J. Rider, A. V. Garcia, M. R. R. Malveira, L. L. Martins, and L. C. M. Direito, "Centralized self-healing scheme for electrical distribution systems," *IEEE Transactions on Smart Grid*, vol. 7, no. 1, pp. 145–155, Jan. 2016.

[11] Y. Li, J. X. Xiao, C. Chen, Y. Tan, and Y. J. Cao, "Service restoration model with mixed-integer second-order cone programming for distribution network with distributed generations," *IEEE Transactions on Smart Grid*, vol. 10, no. 4, pp. 4138–4150, Jul. 2019.

[12] R. Romero, J. F. Franco, F. B. Leão, M. J. Rider, and E. S. De Souza, "A New mathematical model for the restoration problem in balanced radial distribution systems," *IEEE Transactions on Power Systems*, vol. 31, no. 2, pp. 1259–1268, Mar. 2016.

[13] T. S. Bi, Z. Yan, F. S. Wen, Y. X. Ni, C. M. Shen, F. F. Wu, and Q. X. Yang, "On-line fault section estimation in power systems with radial basis function neural network," *International Journal of Electrical Power & Energy Systems*, vol. 24, no. 4, pp. 321–328, May 2002.

[14] T. Z. Yang, W. Y. Chang, and C. L. Huang, "A new neural networks approach to on-line fault section estimation using information of protective relays and circuit breakers," *IEEE Transactions on Power Delivery*, vol. 9, no. 1, pp. 220–230, Jan. 1994.

[15] X. Zhang, S. Yue, and X. B. Zha, "Method of power grid fault diagnosis using intuitionistic fuzzy Petri nets," *IET Generation, Transmission & Distribution*, vol. 12, no. 2, pp. 295–302, Jan. 2018.

[16] B. Falahati, Y. Fu, and L. Wu, "Reliability assessment of smart grid considering direct cyber-power interdependencies," *IEEE Transactions on Smart Grid*, vol. 3, no. 3, pp. 1515–1524, Sep. 2012.

[17] E. Handschin, F. C. Schweppe, J. Kohlas, and A. Fiechter, "Bad data analysis for power system state estimation," *IEEE Transactions on Power Apparatus and Systems*, vol. 94, no. 2, pp. 329–337, Mar. 1975.

[18] M. Beccuti, S. Chiaradonna, F. Di Giandomenico, S. Donatelli, G. Dondossola, and G. Franceschinis, "Quantification of dependencies between electrical and information infrastructures," *International Journal of Critical Infrastructure Protection*, vol. 5, no. 1, pp. 14–27, Mar. 2012.

[19] P. Palensky, E. Widl, and A. Elsheikh, "Simulating cyber-physical energy systems: challenges, tools and methods," *IEEE Transactions on Systems, Man, and Cybernetics*: *Systems*, vol. 44, no. 3, pp. 318–326, Mar. 2014.

[20] M. D. Galus, R. A. Waraich, F. Noembrini, K. Steurs, G. Georges, K. Boulouchos, K. W. Axhausen, and G. Andersson, "Integrating power systems, transport systems and vehicle technology for electric mobility impact assessment and efficient control," *IEEE Transactions on Smart Grid*, vol. 3, no. 2, pp. 934–949, Jun. 2012.

[21] S. J. Xin, Q. L. Guo, H. B. Sun, B. M. Zhang, J. H. Wang, and C. Chen, "Cyber-physical modeling and cyber-contingency assessment of hierarchical control systems," *IEEE Transactions on Smart Grid*, vol. 6, no. 5, pp. 2375–2385, Sep. 2015.

[22] W. X. Liu, Q. Gong, H. Han, Z. Q. Wang, and L. F. Wang, "Reliability modeling and evaluation of active cyber physical distribution system," *IEEE Transactions on Power Systems*, vol. 33, no. 6, pp.7096–7108, Nov. 2018.

[23] D. Ye and T. Y. Zhang, "Summation detector for false data-injection attack in cyber-physical systems," *IEEE Transactions on Cybernetics*, vol. 50, no. 6, pp. 2338–2345, Jun. 2020.

[24] Q. S. Da, L. B. Shi, and Y. X. Ni, "Risk assessment for cyberattack in active distribution systems considering the role of feeder automation," *IEEE Transactions on Power Systems*, vol. 34, no. 4, pp. 3230–3240, Jul. 2019.

[25] X. Zhou, Z. Yang, M. Ni, H. S. Lin, M. L. Li, and Y. Tang, "Analysis of the impact of combined information-physical-failure on distribution network CPS," *IEEE Access*, vol. 8, pp. 44140–44152, Mar. 2020.

[26] C. Lv, W. X. Sheng, K. Y. Liu, and X. Z. Dong, "A novel affine power flow method for improving accuracy of interval power flow data in cyber physical systems of active distribution network," *CSEE Journal of Power and Energy Systems*, Early access in 2021.

[27] W. X. Sheng, K. Y. Liu, and Y. Liang, "Comprehensive fault simulation method in active distribution network with the consideration of cyber security," *IET Cyber-Physical Systems*: *Theory & Applications*, vol. 6, no. 1, pp. 27–40, Mar. 2021.

[28] Y. Liang, M. K. Bai, D. Liu, D. L. Qi, Q. L. Guo, X. S. Ye, T. Y. Kang, H. He, and B. Chai, "A cyber-physical test case for distribution grid operation and control," Early access in 2021.

Wanxing Sheng (SM'13) received the B.Sc., M.Sc., and Ph.D. degrees in Mechanical Engineering from Xi'an Jiaotong University, Xi'an, China, in 1989, 1992, and 1995, respectively. Since 1997, he has been a Full Professor with the China Electric Power Research Institute, Beijing, China, where he is currently the Head of the Department of Power Distribution. He is also a leader of intelligent distribution system and an excellent expert of the State Grid Corporation of China, Beijing. His current research interests include power system analysis, renewable energy generation, and grid-connected technologies. He has published over 150 refereed journal and conference papers, and 15 books.

Keyan Liu (M'13) received the Ph.D. degree in Electrical Engineering from Beihang University, Beijing, China, in 2007. He was a Post-Doctoral Research Fellow with the China Electric Power Research Institute (CEPRI), Beijing, from 2012 to 2014. He is currently a Senior Researcher with CEPRI. His current research interests include distributed generation, planning, and operation analysis of distribution systems, as well as power system computation method and simulation. He has published over 60 refereed journal and conference papers in transactions and journals sponsored by the IEEE, Association for Computing Machinery, and Elsevier.

Zhao Li (S'15–M'21) received B.S. and Ph.D degrees from North China Electric Power University, Beijing, China, in 2015 and 2021. He is currently an engineer in the Distribution Technology Center, China Electric Power Research Institute, Beijing, China. His research interests include digital-analog simulation on the distribution network and distributed power grid.

Xueshun Ye received the M.S. degree from University of Chinese Academy of Sciences, Beijing, in 2013. His research interests include distribution network optimization and simulation.